Article

Formation of Cocrystal Nanorods by Solid-State Reaction of Tetracyanobenzene in 9-Methylanthracene Molecular Crystal Nanorods

Rabih O. Al-Kaysi, Astrid M. Mu#ller, Robert J. Frisbee, and Christopher J. Bardeen

Cryst. Growth Des., **Article ASAP** • DOI: 10.1021/cg800898f • Publication Date (Web): 20 February 2009

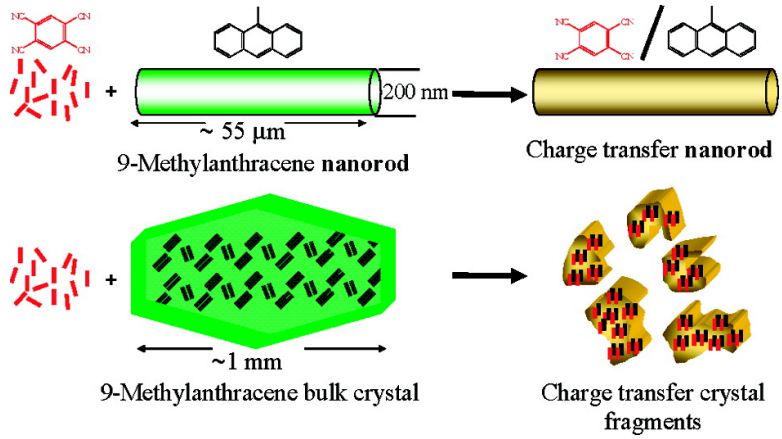

More About This Article

Additional resources and features associated with this article are available within the HTML version:

- Supporting Information
- Access to high resolution figures
- Links to articles and content related to this article
- Copyright permission to reproduce figures and/or text from this article

View the Full Text HTML

CRYSTAL GROWTH & DESIGN
XXXX
VOL. XXX, NO. XX

Formation of Cocrystal Nanorods by Solid-State Reaction of Tetracyanobenzene in 9-Methylanthracene Molecular Crystal Nanorods

Rabih O. Al-Kaysi,[‡] Astrid M. Müller,[§] Robert J. Frisbee, and Christopher J. Bardeen*

Department of Chemistry, University of California, Riverside, California 92521

Received August 15, 2008; Revised Manuscript Received December 20, 2008

ABSTRACT: The reaction of single-component molecular crystal nanorods with a second species to form cocrystal nanorods is described. Single-component crystalline nanorods, composed of 9-methylanthracene (9-MA), are grown in a porous anodic aluminum oxide template. These templated rods are then exposed to a suspension of 1,2,4,5-tetracyanobenzene (TCNB) in water, which slowly diffuses into the 9-MA rods over the course of days. The two species form a 1:1 charge-transfer complex within the rods, which are transformed from crystalline 9-MA into cocrystalline 9-MA/TCNB. The cocrystal nanorods are characterized by electron microscopy, X-ray diffraction, and optical spectroscopy, confirming their highly crystalline structure and the formation of the charge-transfer complex. Attempts to grow cocrystal nanorods directly from a mixed solution were unsuccessful, as were attempts to recreate the single crystal-to-crystal reaction in macroscopic crystals. This work demonstrates how organic nanostructures can support structure-preserving chemical transformations that are impossible in larger crystals.

Introduction

There is currently great interest in both the synthesis and characterization of one-dimensional nanostructures, commonly referred to as nanorods or nanowires. Nanowires composed of inorganic compounds have been grown using a wide variety of methods, and there has also been considerable effort devoted to growing multicomponent or doped inorganic nanostructures.[1] Parallel to efforts in inorganic materials, there has also been progress in making one-dimensional organic nanostructures through both self-assembly methods[2−5] and templated growth.[6−9] For organic nanostructures, the ability to incorporate two different molecular species into a single nanorod would be especially beneficial, since molecular cocrystals can have unique properties relative to single component molecular crystals.[10] Usually such cocrystals are formed by slow precipitation from a mixed solution or slow solvent evaporation, resulting in large crystals. The first examples of nanococrystals were achieved using reprecipitation in conjunction with sonochemistry.[11] Milling (wet or dry)[12−14] can also be used to grow small-scale cocrystals but at the expense of size and shape control. An alternative approach is to first grow a neat crystal of one molecular component with a specified size and shape and then react it with the second component to make a cocrystal that retains the morphology of the original crystal. This approach is not widely used for growing bulk cocrystals due to the scarcity of solid−solid diffusion reactions and problems with strain and crystal disintegration. While surface modification is quite common, chemical transformations occurring within nanostructures are usually limited to rearrangements of the species that are already present, for example, thermal elimination to form new crystal types.[15] Recently, it has been observed that crystalline organic nanostructures undergo various types of photochemical transformations and remain intact, while under identical conditions micron scale or larger crystals will fragment.[16−19] This ability to withstand the strain of phase separation and crystal reconstruction is most likely related to the large surface-to-volume ratio of these small structures, which permits strain relief to occur at the surface in a facile manner.[20] An important question is whether the robustness of organic nanostructures with respect to photochemical transformations, which require only the penetration of photons, extends to chemical processes that require the penetration of molecules into the crystal lattice. If this proves to be the case, then a new class of structure-preserving chemical transformations for organic nanostructures will have been identified.

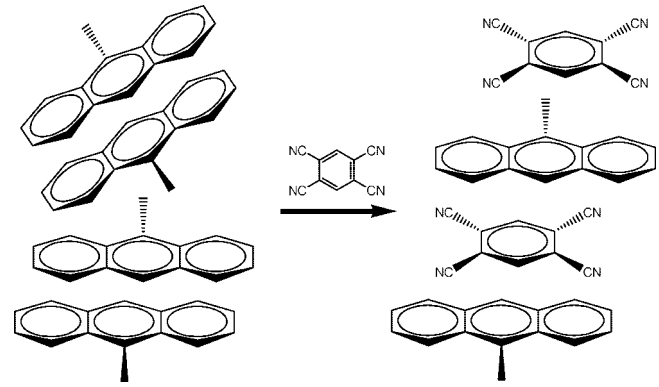

Figure 1. Reactant: Structure of 9-MA with regioregular/herringbone orientation of the units (average distance of 3.8 Å). Product: Structure of the solid diffused 9-MA/TCNB CT cocrystal. The 9-MA maintains its sandwich structure with TCNB inserted in between 9-MA units. Distance between 9-MA and TCNB is 3.6 and 7.3 Å between 9-MA units.

In this paper, we demonstrate that it is indeed possible to grow molecular crystal nanostructures by taking advantage of the crystalline nanorods' ability to retain their morphology during chemical reactions. We examine the reaction of 9-methylanthracene (9-MA) crystalline nanorods with 1,2,4,5-tetracyanobenzene (TCNB) to form a cocrystal with charge-transfer (CT) properties. 9-MA is known to be reactive in its crystalline state,[21,22] and the current reaction, shown in Figure 1, involves

* To whom correspondence should be addressed. E-mail: christopher.bardeen@ucr.edu.
[‡] Current address: Assistant Professor of Chemistry, Department of Basic Sciences, King Saud Bin Abdulaziz University for Health Sciences-National Guard Health Affairs, Building Mail Code 3124, Riyadh 11423, Kingdom of Saudi Arabia.
[§] Current address: Laser Technologist, Beckman Institute Staff, California Institute of Technology, Mail Code 139-74, Pasadena, California 91125.

10.1021/cg800898f CCC: $40.75

a crystal-to-crystal transformation that occurs within the channels of a porous anodic aluminum oxide (AAO) template. In the case of 9-MA/TCNB cocrystal the driving force behind the solid−solid diffusion reaction is the formation of the thermodynamically stable ground-state charge-transfer complex. 9-MA is a good electron donor to the strong electron acceptor TCNB. The formation of ground-state charge-transfer complexes is typical for electron-rich planar polycyclic aromatic hydrocarbons (PAH) and planar electron acceptors such as TCNB.[23,24] Organic charge-transfer nanorods have been previously synthesized using single component templated growth,[25] electric-field methods,[26−28] and photocrystallization.[29] Our new approach demonstrates that it is possible to completely react a homogeneous nanorod with a second molecular species without disrupting its morphology. Furthermore, we show that this approach only works with nanostructures: attempting to apply the same method to macroscopic crystals leads to morphology changes and eventually fragmentation. The present work demonstrates how organic nanostructures provide new opportunities for doing solid-state chemistry in a controlled way, for example, the growth nanoscale molecular cocrystals with well-defined shapes and sizes.

Experimental Procedures

Synthesis of 9-MA/TCNB Charge-Transfer Nanorods. Twelve milligrams of 9-methylanthracene (9-MA) was dissolved in 0.1 mL of dry tetrahydrofuran (THF). The solution was deposited on the surface of an AAO template (Whatman Anodisc-13, 200 nm pore diameter, average membrane thickness of 60 μm, membrane diameter of 25 mm, with polypropylene supporting ring). The loaded AAO template was placed on a homemade Teflon holder that suspends it from the polymer support ring. The holder was then placed in a 16 oz glass jar containing 2 mL of THF and a 1 in. ring of filter paper to disperse the solvent vapors. The jar was tightly covered and a long needle was inserted through the cover till it touched the bottom of the jar. Another needle was inserted in the cover and was coupled with a gas bubbler. Argon gas was gently introduced into the jar at a rate of 1 bubble every 2 s. The slow room temperature vapor solvent annealing causes the 9-MA in the Anodisc to dissolve in the solvent vapors and slowly crystallize in the AAO template pores to form single crystalline nanorods. After all the solvent had evaporated, the solvent annealed AAO template was polished using 2000 grit sandpaper to remove excess 9-MA from the surface. Twenty milligrams of 1,2,4,5-tetracyanobenzene (TCNB) was sonicated in 20 mL of distilled water to form a suspension (TCNB is slightly water soluble). The 9-MA loaded AAO template is immersed in the TCNB/water suspension and sonicated for several seconds to clear the surface of the template from air bubbles and initiate "wetting" of the surface. The surface of the AAO template immediately turns red indicating the formation of the CT complex. The mixture was left undisturbed in a dark place at room temperature for 3 weeks for maximum conversion, while excess TCNB precipitates out and evenly coats the top of the AAO template. The loaded AAO template was given a brief polish with 2000 grit sandpaper. The cocrystal nanorods are liberated by dissolving the AAO template in 50% aqueous H_3PO_4. Excess unconverted 9-MA was extracted by shaking the aqueous suspension of the CT nanorods with hexane. The CT complex behaves like an organic salt and has negligible solubility in hexane or water. The CT nanorods were stored in deionized water.

Synthesis of Large 9-MA/TCNB Cocrystals. TCNB (0.0505 g, 2.80×10^{-4} mol) was dissolved in 0.5 mL of THF. To this solution was added 9-MA (0.0540 g, 2.81×10^{-4} mol) dissolved in 0.3 mL of THF. The solution mixture turns deep red followed by the precipitation of red CT crystals. The solvent was allowed to slowly evaporate at room temperature. The crystals obtained were of high enough quality to enable structure determination by X-ray diffraction (XRD) (Supporting Information CIF file and Tables 1−6).

Synthesis of 9-MA/TCNB Bulk Cocrystal Powder via Wet Milling. TCNB (0.2 g, 0.0011 mol) was added to 9-MA (0.211 g, 0.0011 mol) along with a couple of drops of water in an agate mortar. The mixture was milled until a red paste formed. Water was periodically added to prevent the paste from drying. A total of 30 min of mixing time was performed. The wet paste was stored in the dark for several days to allow complete diffusion of the components.

AFM Measurement of the 9-MA Crystal Surface. To examine the topology 9-MA single crystal before and after exposure to TCNB, we used a Novascan AFM mounted on top of an Olympus IX-70 inverted fluorescence microscope. A flat single crystal of 9-MA with 2×1.5 mm dimensions (grown by slow evaporation of a 9-MA THF solution) was placed on a microscope slide using a small amount of silicon grease as an adhesive. An intermittent contact (tapping) mode scan was performed to minimize any physical contact with the sample which might cause it to shift position on the surface. The pristine 9-MA surface was scanned first. The tip of the AFM was gently withdrawn to expose the surface of the 9-MA crystal. A drop of clear saturated TCNB/water solution was carefully deposited on the 9-MA crystal surface and left for 3 min, after which the excess solution was gently washed away with distilled water and air-dried. The AFM tip was lowered back to the same approximate region and scanning commenced.

Absorption and Fluorescence Spectra. We could not directly measure the absorption spectra of the 9-MA and 9-MA/TCNB nanorods because of small sample volumes and scattering. In most cases, the fluorescence excitation spectrum is a good representation of the absorption. Both the emission and excitation spectra were collected using front-face geometry in a Spex Fluorolog fluorimeter. The nanorods were left in the alumina template to provide a flat, low-scattering surface normal to the exciting beam. The fluorescence spectra were collected using 365 and 500 nm excitation wavelengths for the 9-MA and 9-MA/TCNB nanorods, respectively. The excitation spectra were measured using detection wavelengths of 550 and 650 nm for the 9-MA and 9-MA/TCNB nanorods, respectively. Note that care was taken to minimize the exposure of the 9-MA samples to UV light, since 9-MA is known to undergo a solid-state [4 + 4] photodimerization.[30] The 9-MA solid fluorescence was observed to slowly disappear under UV irradiation, in contrast to the 9-MA/TCNB cocrystal, which was completely photostable.

SEM and TEM. For the SEM measurements a drop of the aqueous CT nanorod suspension was placed on a copper tape and fixed on an SEM stub. The water was gently evaporated leaving behind dispersed bundles of nanorods. The SEM stub was sputter coated with Pt/Au for a cycle of 60 s. The SEM stub was placed inside a scanning electron microscope (XL30 FEG) and the data were collected using a 10 kV electron beam. Transmission electron microscopy of the nanorods was performed using a FEI-PHILIPS CM300 model. The specimen was prepared by depositing a drop of the aqueous 9-MA/TCNB nanorod suspension on the graphite grid sample holder and gently dried. Note that we were not able to perform electron microscopy measurements on pure 9-MA nanorods because the 9-MA rapidly sublimes under high vacuum and electron beam heating.

Powder X-ray Diffraction. All measurements were performed using a Bruker D8 Advance diffractometer with Cu Kα radiation (40 kV, 40 mA, $\lambda = 1.5418$ Å). In all cases a background scan of the polycarbonate sample holder was first performed. Then hexane extracted CT nanorods were scattered on the sample holder (without moving it) and scanned over a wide angle, typically between 5 and 70 deg at a scan rate of 0.1 deg/s. The calculated powder XRD of the CT nanorods was generated using the Mercury 1.4.2 program (Supporting Information).

Results and Discussion

The molecular cocrystal nanorods were formed using a variant of the solvent-annealing process developed by us previously to grow nanorods out of a variety of molecules.[31] The procedure is outlined in Figure 2. After solvent annealing in the pores of an AAO template, 9-MA molecular crystal nanorods are formed. Excess 9-MA on the template surface is removed by polishing. Then an aqueous suspension of TCNB is deposited on the template and the sample is left in a sealed container for a period of several weeks. During this time, the TCNB slowly diffuses along the length of the channel, converting the 9-MA crystal into a 9-MA/TCNB cocrystal. The conversion is rarely 100% along the whole length of the rod, as judged from the fluorescence images. Even after a period of three weeks some unreacted 9-MA is left at the tip or along the length of the

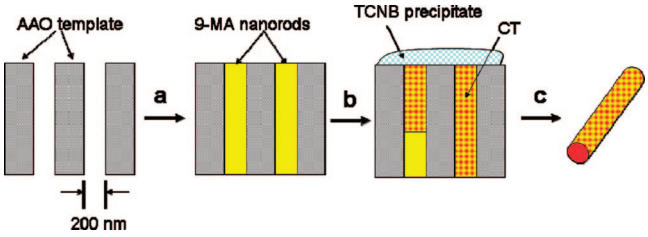

Figure 2. (a) 9-MA solution in THF was deposited on AAO and solvent annealed to produce 9-MA nanorods. (b) TCNB suspension in water was deposited on the surface of the 9-MA loaded AAO and allowed to diffuse in to form the CT complex for several days. (c) The alumina template was removed by dissolving it in 50% phosphoric acid. Excess unconverted 9-MA can be washed away with hexane without dissolving the CT nanorods.

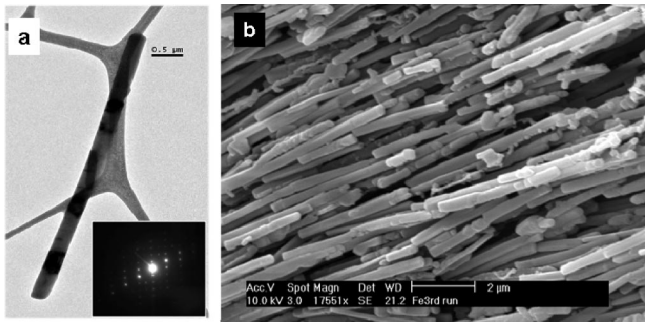

Figure 3. (a) TEM of 9-MA/TCNB CT nanorod. The different shades of the nanorod are caused by the reflection of the electron beam off crystalline planes, an indication of the homocrystallinity of the nanorod. Inset: Electron diffraction of the CT nanorod with discreet diffraction pattern. (b) SEM of hexane washed CT nanorods.

nanorod. If the reaction is interrupted, one can observe a sharp (<1 μm wide) boundary between the unreacted 9-MA and 9-MA/TCNB cocrystal regions along the rod by fluorescence microscopy. In cases where partially converted 9-MA and CT nanorods were investigated by TEM, electron beam heating would sublime out the unreacted 9-MA part of the nanorod, leaving behind a submicron boundary of the cocrystal regions. Thus, the reaction seems to occur via a well-defined diffusion front that slowly advances along the rod.[32] The larger volume of the cocrystal results in extra CT material that is extruded from the pores and deposited on the template surface. In general, this red solid on the surfaces is mixed with unreacted TCNB and attempts to quantify the amount of extruded cocrystal were unsuccessful. It should be emphasized that this material must contain both 9-MA and TCNB, since its optical properties are consistent with the CT complex described below. Thus, 9-MA is displaced by the TCNB within the template, as expected.

The AAO template can be dissolved in a strong acid solution and the properties of the isolated rods examined in detail. The structural properties of the nanorods have been characterized using a variety of methods. The cocrystal rods are more fragile than the 9-MA rods (just as the bulk cocrystals are more brittle than bulk 9-MA crystals) and tend to break under prolonged electron beam illumination, but their rod morphology is clearly seen using electron microscopy. In Figure 3a we show the TEM image of a single rod segment on the graphite membrane substrate. The inset of Figure 3a shows the electron diffraction pattern obtained from this rod (Supporting Information, Figure 2). The discrete spots and oriented pattern indicate the presence of a single crystalline domain within the electron beam focus (~1 μm) in diameter. From this data, we estimate that single

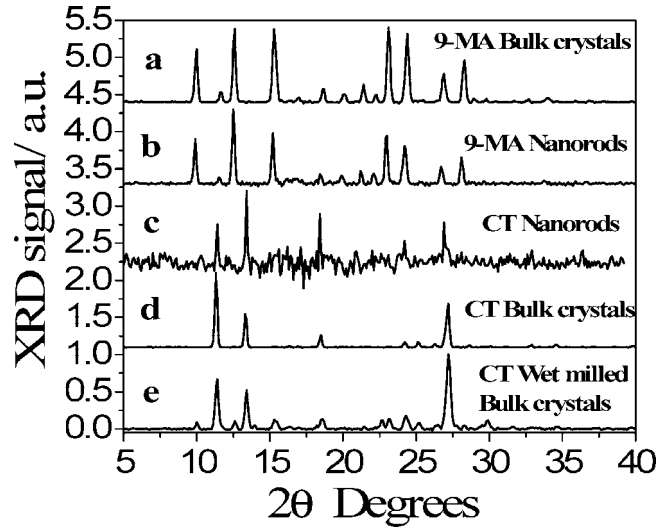

Figure 4. (a) Powder XRD of bulk 9-MA crystals. (b) Powder XRD of 9-MA nanorods. (c) Powder XRD of 9-MA/TCNB cocrystal nanorods. The low signal-to-noise is due to the small amount of sample used. (d) Powder XRD of bulk 9-MA/TCNB cocrystals obtained by mixing 9-MA and TCNB in THF and filtering the precipitated solid. (e) Powder XRD of bulk 9-MA/TCNB cocrystals obtained by wet milling a mixture of 9-MA and TCNB. Result similar to dry milling.

cocrystal domains on the order of microns are formed by the reaction with TCNB. The different shades of the nanorod are caused by the reflection of the electron beam off crystalline planes, an indication of the homocrystallinity of the nanorod. Note that if the reaction did not penetrate through the nanorod, or if there were significant regions of unreacted 9-MA, we would expect the TEM electron diffraction pattern to broaden and yield rings instead of spots. Also, when the reacted rod is examined under high vacuum in the TEM, we do not see evidence of disruption that would be caused by sublimation of unreacted 9-MA. The SEM image in Figure 3b shows a collection of cocrystal nanorods deposited on a glass surface. The rod morphology is clearly preserved, although the surface appears slightly roughened, perhaps due to residual strain induced by the reaction (see discussion below).

Further evidence for the crystalline nature of the rods is provided by powder XRD experiments. In Figure 4a,b, we show the powder XRD patterns of the 9-MA bulk crystals[30] and 9-MA nanorods, respectively. The excellent correlation between the peaks is evidence of the crystalline nature of the 9-MA nanorods. The methyl units in 9-MA are arranged in a head to tail fashion with the anthracene units assuming a sandwich herringbone motif. After the nanorods are reacted with TCNB, the new pattern in Figure 4c is obtained. These new peaks line up with those from a bulk cocrystal powder obtained by either solution growth (Figure 4d) or by wet milling (Figure 4e). The relative peak intensities are different, possibly due to residual crystal alignment in the nanorod sample. Another possible complication is that in the solution-grown cocrystal the head-to-tail orientation of the 9-MA methyl groups is random, most likely because the extra separation introduced by the presence of the TCNB lessens the steric interactions between these methyl groups. This random orientation is not expected in the cocrystals grown directly from the 9-MA crystal, where the methyl orientations start out fixed in an alternating pattern. But comparison of the wet-milled and solution-grown bulk cocrystals in Figure 4d,e show no discernible difference in the powder XRD patterns between the two, suggesting that any ordering of the 9-MA methyls cannot be

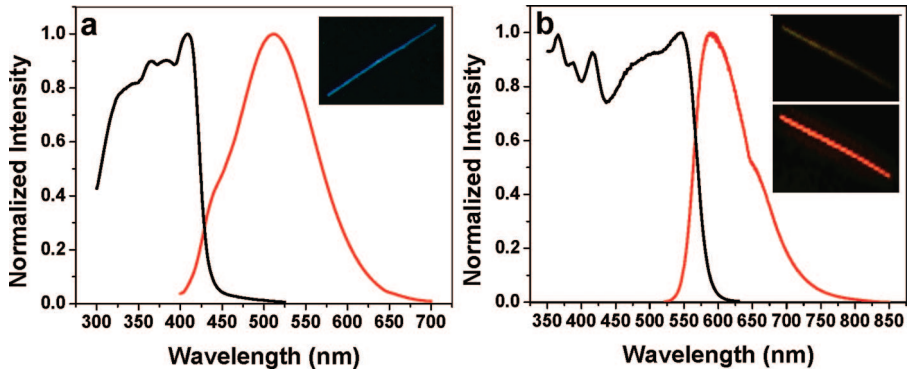

Figure 5. (a) Excitation (black) and fluorescence (red) spectra of 9-MA nanorods. Inset: Fluorescence image of a 200 nm diameter 9-MA nanorod excited with 365 nm light. (b) Excitation (black) and fluorescence (red) spectra of the 9-MA/TCNB cocrystal nanorods. Inset: a single 200 nm diameter cocrystal nanorod excited with 365 nm (upper inset), and excited with 500 nm (lower inset) where the CT complex has a strong absorption. In all the fluorescence images, the rod length is ~50 μm.

discerned at this level of analysis. The important point is that the data in Figure 4, especially the narrow XRD peakwidths and good correspondence of the nanorod peaks to the bulk crystal peaks, provide strong evidence for the crystal-to-crystal nature of the reaction in the nanorods.

The change in crystal structure is accompanied by a change in optical properties. We were unable to directly measure the absorption of the nanorod samples due to strong light scattering in both transmission and reflection geometries. Fluorescence excitation spectra can be obtained more easily, but in this case self-absorption effects can complicate interpretation of the results.[33,34] These effects are minimized by using front-face detection and, for excitation measurements, detecting at an emission wavelength far from the absorption edge. While we cannot rule out residual distortion of the spectra due to wavelength-dependent absorption and scattering in our solid samples, the close agreement of our excitation spectrum of 9-MA rods with absorption spectra of ultrathin spin cast 9-MA films suggests that such effects are minor. Figure 5a shows the excitation and fluorescence spectra of 9-MA nanorods, along with a fluorescence microscope image of a single rod. The structured excitation spectrum beginning at around 420 nm and the featureless excimer emission at 500 nm are both consistent with previous measurements on bulk 9-MA crystals.[35] For the cocrystals, a new excitation peak appears at around 520 nm, while the fluorescence peak is shifted to 610 nm. The red shift and broadening are typical of CT absorption lineshapes and reflects the increased coupling of this transition to environmental vibrational degrees of freedom.[36,37] The spectroscopic data are consistent with a change from a neutral excited-state in the 9-MA crystal to a CT excited-state in the 9-MA/TCNB cocrystal. This is expected since TCNB forms a CT complex with a variety of anthracene derivatives.[24,38] The fluorescence we observe is consistent with that previously observed for both anthracene and 9-MA complexes with TCNB.[39,40] The change in optical properties is immediately apparent by observing the nanorods with a fluorescence microscope, where the blue-green 9-MA rods change to the red-emitting CT rods.

We have shown how the 9-MA/TCNB cocrystal nanorods can be grown from pristine 9-MA crystalline nanorods. Normally, macroscopic cocrystals would be grown by precipitation from a mixed solution of 9-MA and TCNB. We attempted to use this mixed solution method for templated growth of cocrystal nanorods in a single step. After solvent annealing using an equimolar mixed solution of 9-MA and TCNB, we find that no rods are formed, although bulk cocrystals form on the surface of the AAO membrane. The low solubility of the CT complex in organic solvents such as THF prevents its dissolution in the solvent vapor which is necessary for crystal restructuring during the solvent annealing process.[31] Instead of growing nanorods, we can try to use the same reaction conditions for our nanorods to transform bulk 9-MA crystals into bulk cocrystals. In this case, the reaction is successful, but the structural integrity of the macroscopic crystal is lost. The TCNB diffuses into the bulk crystal, but the crystal quickly disintegrates. The effect of TCNB exposure on a pristine 9-MA crystal can be seen in Figure 6, which shows an AFM image of the crystal surface before and after exposure to a saturated aqueous solution of TCNB. The 9-MA crystal exhibits some 8−10 nm periodic ridges before exposure, but is otherwise featureless. After exposure, the surface undergoes dramatic changes, with eruptions that extend hundreds of nanometers above the surface. This type of surface roughening has been previously observed for 9-MA and other molecular crystals reacting with gases[41,42] and undergoing photochemical reactions[43] and has been ascribed to strain buildup between the heterogeneous phases within the crystal during the reaction.

It has been shown that the overall process of guest transport in a van der Waals molecule crystal to form a new intact crystals requires extensive cooperativity among the host molecules.[44] It is possible that the presence of water aids the penetration of TCNB into the 9-MA crystal, but the fact that we could successfully make cocrystals by dry milling the two solids together shows that the presence of water is not required. The surface roughening observed in our AFM experiments suggests that the formation of the 9-MA/TCNB cocrystal does lead to significant strain within the crystal. Obviously some morphologies (e.g., macroscopic crystals) cannot accommodate this strain. One explanation for why the nanocrystals remain intact is that their high surface-to-volume ratios permit the strain to be alleviated at the crystal surface. While all previous examples of this size effect have centered on photochemical reactions, the present work demonstrates that bimolecular reactions can benefit from it as well. There are other factors that may also be important. Our reactions were carried out with the 9-MA rods still confined within the AAO template. It is possible that the template itself forces the nanorod to remain intact during the reaction. To examine the role of the template, we have reacted aqueous 9-MA nanorod suspensions with aqueous TCNB. 9-MA/TCNB nanorods form and remain intact even without the template, but tend to be much more heterogeneous, with 9-MA and 9-MA/TCNB regions highly intermixed. This

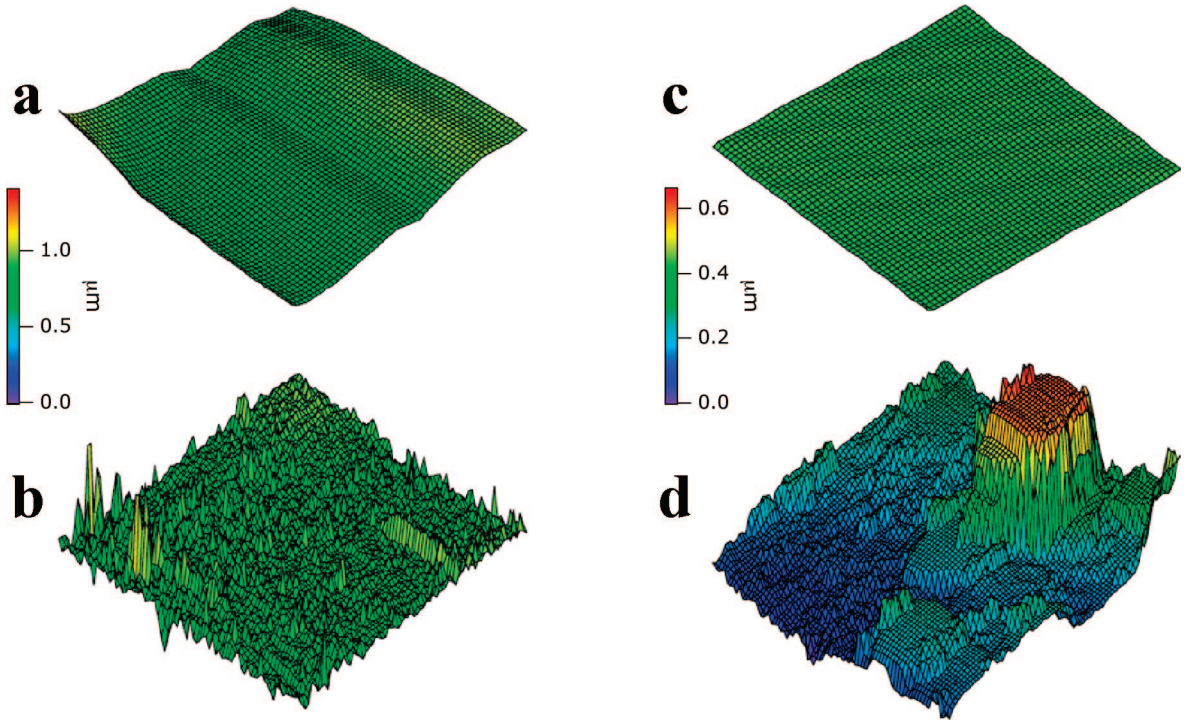

Figure 6. AFM height image using tapping mode of the surface of a solution grown 9-MA crystal before and after adding an aqueous solution of TCNB. (a) An 80 μm by 80 μm scan of the surface of 9-MA crystal. (b) The same surface after 3 min exposure to a saturated aqueous TCNB solution. (c) A 10 μm by 10 μm scan of 9-MA surface. (d) The same surface after a 3 min exposure to saturated aqueous TCNB solution.

uncontrolled diffusion approach demonstrates that confinement is not necessary for the structure-preserving reaction in the nanorods, but it also resulted in more disordered samples and therefore was not pursued. A third possibility is that anisotropic diffusion within the nanorods helps them remain intact. The rate of molecular diffusion within a crystal is known to depend on the crystal axis,[45,46] and it is possible that the crystal orientation of 9-MA in the rod, with only the ends exposed to TCNB, favors diffusion along a slow axis, which would lead to more gradual conversion and less fracture. Again, our results on the free rods suggest that even without constraints on the TCNB access to the rods, the rods can incorporate the TCNB and remain intact, albeit with less uniform reaction.

Conclusion

In this paper, we demonstrate a novel way to grow nanostructured molecular cocrystals. By taking templated nanorods of 9-MA and exposing them to aqueous suspensions of TCNB, we can form the 9-MA/TCNB cocrystal while retaining the structural integrity of the rods. The morphology of the cocrystal rods is characterized by electron microscopy and X-ray diffraction, while their charge-transfer nature is confirmed by optical spectroscopy. It is important to stress that this crystal-to-crystal reaction is the only route to the CT crystal nanorods, since nanorod growth from a mixed solution leads to phase separation and formation of random crystals on the surface of the template, while attempting to reproduce the reaction in bulk crystals leads to fragmentation. The use of nanostructured molecular crystals may provide opportunities for performing morphology-preserving chemical transformations that cannot be achieved in bulk crystals. Preliminary results in our laboratory suggest that TCNB cocrystal nanorods can be grown using the same method with different anthracene derivatives, including 9-anthracene carboxylic acid and 9-*tert*-butyl anthracene ester, as well as using different diameter templates. Our previous work has shown how single-component molecular crystal nanorods can exhibit interesting photomechanical properties, and the present work may lead to nanowires with interesting optoelectronic and electronic properties. Taken together, these results suggest that molecular crystal nanostructures provide a fruitful area for the exploration of solid state chemical reactivity.

Acknowledgment. C.J.B. acknowledges the support of the National Science Foundation, Grant CHE-0719039, and the University of California Energy Institute. The authors are pleased to acknowledge Professor P. Feng of the University of California, Riverside, for access to the XRD instrument. Electron microscopy measurements on the nanorods were performed at the Central Facility for Advanced Microscopy and Microanalysis (CFAMM) at UCR.

Supporting Information Available: Calculated powder XRD of the CT complex. TEM and SEM of CT nanorods. Crystal structure table of the CT complex. This information is available free of charge via the Internet at http://pubs.acs.org.

References

(1) Law, M.; Goldberger, J.; Yang, P. Semiconductor nanowires and nanotubes. *Ann. Rev. Mater. Res.* **2004**, *34*, 83–122.
(2) Loi, S.; Wiesler, U.-M.; Butt, H.-J.; Mullen, K. Formation of nanorods by self-assembly of alkyl-substituted polyphenylene dendrimers on graphite. *Chem. Comm.* **2000**, 1169–1170.
(3) Liu, H.; Li, Y.; Xiao, S.; Gan, H.; Jiu, T.; Li, H.; Jiang, L.; Zhu, D.; Yu, D.; Xiang, B.; Chen, Y. Synthesis of organic one-dimensional nanomaterials by solid-phase reaction. *J. Am. Chem. Soc.* **2003**, *125*, 10794–10795.
(4) Schiek, M.; Balzer, F.; Al-Shamery, K.; Brewer, J. R.; Lutzen, A.; Rubahn, H. G. Organic molecular nanotechnology. *Small* **2008**, *4*, 176–181.
(5) Briseno, A. L.; Mannsfeld, S. C. B.; Reese, C.; Hancock, J. M.; Xiong, Y.; Jenekhe, S. A.; Bao, Z.; Xia, Y. Perylenediimide nanowires and their use in fabricating field-effect transistors and complementary inverters. *Nano Lett.* **2007**, *7*, 2847–2853.

(6) Qu, L.; Shi, G. Crystalline oligopyrene nanowires with multicolored emission. *Chem. Comm.* **2004**, 2800–2801.
(7) Gan, H.; Liu, H.; Li, Y.; Liu, Y.; Lu, F.; Jiu, T.; Zhu, D. Template synthesis and characterization of chiral organic nanotubes and nanowires. *Chem. Phys. Lett.* **2004**, *399*, 130–134.
(8) Jiang, L.; Fu, Y.; Li, H.; Hu, W. Single-crystalline, size and orientation controllable nanowires and ultralong microwires of organic semiconductor with strong photoswitching property. *J. Am. Chem. Soc.* **2008**, *130*, 3937–3941.
(9) Thomas, A.; Goettmann, F.; Antonietti, M. Hard templates for soft materials: creating nanostructured organic materials. *Chem. Mater.* **2008**, *20*, 738–755.
(10) Braga, D.; Grepioni, F. Making crystals from crystals: a green route to crystal engineering and polymorphism. *Chem. Commun.* **2005**, 3635–3645.
(11) Bucar, D. K.; MacGillivray, L. R. Preparation and reactivity of nanocrystalline cocrystals formed via sonocrystallization. *J. Am. Chem. Soc.* **2007**, *129*, 32–33.
(12) Horn, D.; Rieger, J. Organic nanoparticles in the aqueous phase−theory, experiment and use. *Angew. Chem., Int. Ed.* **2001**, *40*, 4330–4361.
(13) Kuroda, R.; Imai, Y.; Tajima, N. Generation of a co-crystal phase with novel coloristic properties via solid state grinding procedures. *Chem. Commun.* **2002**, 2848–2849.
(14) Braga, D.; Maini, L.; Polito, M.; Mirolo, L.; Grepioni, F. Assembly of hybrid organic-organometallic materials through mechanochemical acid-base reactions. *Chem. Eur. J.* **2003**, *9*, 4362–4370.
(15) Du, N.; Zhang, H.; Chen, B.; Wu, J.; Li, D.; Yang, D. Low temperature chemical reaction synthesis of single-crystalline $Eu(OH)_3$ nanorods and their thermal conversion to Eu_2O_3 nanorods. *Nanotechnology* **2007**, *18*, 065605/1−065605/4.
(16) Takahashi, S.; Miura, H.; Kasai, H.; Okada, S.; Oikawa, H.; Nakanishi, H. Single-crystal-to-single-crystal transformation of diolefin derivatives in nanocrystals. *J. Am. Chem. Soc.* **2002**, *124*, 10944–10945.
(17) Al-Kaysi, R. O.; Muller, A. M.; Bardeen, C. J. Photochemically driven shape changes of crystalline organic nanorods. *J. Am. Chem. Soc.* **2006**, *128*, 15938–15939.
(18) Al-Kaysi, R. O.; Bardeen, C. J. Reversible photoinduced shape changes of crystalline organic nanorods. *Adv. Mater.* **2007**, *19*, 1276–1280.
(19) Al-Kaysi, R. O.; Dillon, R. J.; Kaiser, J. M.; Mueller, L. J.; Guirado, G.; Bardeen, C. J. Photopolymerization of organic molecular crystal nanorods. *Macromolecules* **2007**, *40*, 9040–9044.
(20) Colombier, I.; Spagnoli, S.; Corval, A.; Baldeck, P. L.; Giraud, M.; Leaustic, A.; Yu, P.; Irie, M. Diarylethene microcrystals make directional jumps upon ultraviolet irradiation *J. Chem. Phys*. **2007**, *126*, 011101/1−011101/3.
(21) Pratt, E. F.; Trapasso, L. E. The autoxidation of selected organic solids in the presence of alumina. *J. Am. Chem. Soc*. **1960**, *82*, 6405–6408.
(22) Watanabe, H.; Senna, M. Acceleration of solid state Diels-Alder reactions by incorporating the reactants into crystalline charge transfer complexes. *Tetrahedral Lett.* **2005**, *46*, 6815–6818.
(23) Foster, R.; Thomson, T. J. Interaction of electron acceptors with bases. Part 10. Complexes of polycyanobenzenes with electron donors. *Trans. Farad. Soc.* **1963**, *59*, 2287–2295.
(24) Wright, J. D. *Molecular Crystals*, 2nd ed.; Cambridge University Press: Cambridge, 1995.
(25) Zhang, X.; Xhang, X.; Zou, K.; Lee, C.-S.; Lee, S.-T. Single-crystal nanoribbons, nanotubes, and nanowires from intramolecular charge-transfer organic molecules. *J. Am. Chem. Soc.* **2007**, *129*, 3527–3532.
(26) Sakai, M.; Iizuka, M.; Nakamura, M.; Kudo, K. Self-organized growth of tetrathiafulvene-tetracyanoquinodimethane molecular wires using the coevaporation method under a static electric field. *J. Appl. Phys*. **2005**, *97*, 053509/1−053509/4.
(27) Nafady, A.; Bond, A. M.; Bilyk, A.; Harris, A. R.; Bhatt, A. I.; O'Mullane, A. P.; Marco, R. D. Tuning the electrocrystallization parameters of semiconducting $Co(TCNQ)_2$-based materials to yield either single nanowires or crystalline thin films. *J. Am. Chem. Soc.* **2007**, *129*, 2369–2382.
(28) Savy, J.-P.; Caro, D. d.; Faulmann, C.; Valade, L.; Almeida, M.; Koike, T.; Fujiwara, H.; Sugimoto, T.; Fraxedas, J.; Ondarcuhu, T.; Pasquier, C. Nanowires of molecule-based charge-transfer salts. *New J. Chem.* **2007**, *31*, 519–527.
(29) O'Mullane, A. P.; Fay, N.; Nafady, A.; Bond, A. M. Preparation of metal-TCNQ charge-transfer complexes on conducting and insulating surfaces by photocrystallization. *J. Am. Chem. Soc.* **2007**, *129*, 2066–2073.
(30) Turowska-Tyrk, I.; Trzop, E. Monitoring structural transformations in crystals. 6. The [4 + 4] photodimerization of 9-methyl-anthracene. *Acta Crystallogr. B* **2003**, *59*, 779–786.
(31) Al-Kaysi, R. O.; Bardeen, C. J. General method for the synthesis of crystalline organic nanorods using porous alumina templates. *Chem. Commun.* **2006**, 1224–1226.
(32) Rastogi, R. P.; Bassi, P. S.; Chadha, S. L. Kinetics of reaction between naphthalene and picric acid in the solid state. *J. Phys. Chem.* **1962**, *66*, 2707–2708.
(33) Birks, J. B. *Photophysics of Aromatic Molecules*; Wiley & Sons: London, 1970.
(34) Mammel, U.; Brun, M.; Oelkrug, D. Absorption and emission spectroscopy in scattering media: modelling of fluorescence decay curves and photometric laws for systems with inhomogeneous absorber distribution. *Fresenius J. Anal. Chem* **1992**, *344*, 147–152.
(35) Cohen, M. D.; Ludmer, Z.; Yakhot, V. The fluorescence properties of crystalline anthracenes and their dependence on crystal structures. *Phys. Status Solidi B* **1975**, *67*, 51–61.
(36) Marcus, R. A. On the theory of shifts and broadening of electronic spectra of polar solutes in polar media. *J. Chem. Phys.* **1965**, *43*, 1261–1274.
(37) Cortes, J.; Heitele, H.; Jortner, J. Band-shape analysis of the charge-transfer fluorescence in barrelene-based electron-donor-acceptor compounds. *J. Phys. Chem.* **1994**, *98*, 2527–2536.
(38) Tsuchiya, H.; Marumo, F.; Saito, Y. The crystal structure of the 1:1 complex of anthracene and 1,2,4,5-tetracyanobenzene. *Acta Crystallogr. B* **1972**, *28*, 1935–1941.
(39) Zhou, J.; Zhong, C.; Francis, T. M.; Braun, C. L. Radiative exciplexes of 1,2,4,5-Tetracyanobenzene with sterically hindered alkylbenzenes. *J. Phys. Chem. A* **2003**, *107*, 8319–8326.
(40) Hosaka, N.; Obata, M.; Suzuki, M.; Saiki, T.; Takeda, K.; Kuwata-Gonokami, M. Nanosized crystallites of charge-transfer complex of 9-methylanthracene and 1,2,4,5-tetracyanobenzene for bright and optically anisotropic fluorescent probes. *Appl. Phys. Lett.* **2008**, *92*, 113305/1−113305/3.
(41) Kaupp, G.; Schmeyers, J. Gas/solid reactions with nitrogen dioxide. *J. Org. Chem.* **1995**, *60*, 5494–5503.
(42) Kaupp, G.; Herrmann, A.; Schmeyers, J. Waste-free chemistry of diazonium salts and benign separation of coupling products in solid state reactions. *Chem. Eur. J.* **2002**, *8*, 1395–1405.
(43) Kaupp, G. Photodimerization of anthracenes in the solid state: new results from atomic force microscopy. *Angew. Chem., Int. Ed.* **1992**, *31*, 595–598.
(44) Atwood, J. L.; Barbour, L. J.; Jerga, A.; Schottel, B. L. Guest transport in a nonporous organic solid via dynamic van der Waals cooperativity. *Science* **2002**, *298*, 1000–1002.
(45) Bonpunt, L.; Dautant, A.; Loumaid, A.; Faure, F. 2-Naphthol lattice diffusion at infinite dilution in naphthalene single crystals. I. Diffusion tensor - influence of the purity of the naphthalene. *J. Phys. Chem. Solids* **1989**, *50*, 777–783.
(46) Cvetkovic, A.; Picioreanu, C.; Straathof, A. J. J.; Krishna, R.; van der Wielen, L. A. M. Relation between pore sizes of protein crystals and anisotropic solute diffusivities. *J. Am. Chem. Soc.* **2005**, *127*, 875–879.

CG800898F